http://dx.doi.org/10.21611/qirt.2008.10_06_07

Two-dimensional thermal analysis of organic materials by micro-scale thermography

by J. Morikawa*, E. Hayakawa***, T.Eto**, T. Hashimoto*

*Tokyo Institute of Technology, O-okayama, Meguro-ku,Tokyo 152-8550, Japan
** Eto Denki,Co. Ltd., Shinkawa, Mitaka, Tokyo 181-0004, Japan
*** ai-Phase, Co. Ltd., Osaki, Shinagawa, Tokyo 141-0061, Japan

Abstract

.

n– alkanes have been widely studied as a model material of lipids, liquid crystals, fatty acids, the cell membrane, and polymers. It is known that its complicated phase transition corresponds to the functions of these materials. The methods of X-ray diffraction, IR spectroscopy, and DSC (Differential scanning calorimetry) are generally used to study the phase transitions of *n*- alkanes, however, few thermo-graphical measurements have been done. This study gives a new observation on phase transitions and structure formation processes of *n*-alkane by using a high-speed IR camera with an InSb focal plane arrays on the basis of a method of micro-scale two-dimensional thermal analysis. The advantage of this technique is a micro-scale spatial resolution (3μm) and a high-speed data storage. The forerunning phenomenon of phase transition was visualized as the spatial temperature fluctuation by a two-dimensional differential calculus. The differences of the spatial inhomogeneity of proceeding speed of crystallization and rotator phase transitions were analyzed on *n*- pentacosane, *n*-tetracosane, and *n*- tricosane.

1. Introduction

The odd and even number effect of phase behaviour of organic molecular crystals of *n*- alkanes has been investigated in detail by various measuring techniques for its importance as a model material of a functional device in electronic industry, or as a model of a phospholipids bilayer and fatty acids in biophysical sciences. However, the heat transport properties such as thermal diffusivity and thermal conductivity of *n*- alkanes in solid-solid phase transition and crystallization under the exothermic latent heat have not yet been sufficiently studied.

Two-dimensional micro scale thermal analysis [1-4] for the measurement of latent heat that is released from the freezing biological cells was examined in detail by use of a high-speed and micro-scale IR imaging technique. The thermo graphically observed latent heat that is spreading over the tissues allow estimating the thermal properties of the cell membrane and a heat source.

The magnification factor of the IR micro-lens and the data-capturing/storage speed are improved in this study. The quantitative thermal analysis of an odd and an even number *n*- alkane under a temperature scan is examined, which introduces a new insight in the micro-scale thermal analysis of the early stage of crystallization and phase transitions of *n*- alkane from the viewpoint of heat transfer and its relationships with the structure appearances.

2. Experimental

2.1. IR thermography

A high-speed IR camera, Phoenix (Indigo), having an indium-antimony (InSb) sensor array of 320x256 pixels with the optimum wavelength between 3μm and 5μm, was used for taking the micro-scale thermography with the originally designed silicon germanium made microscopic lens with a magnification of x10, x7 and x1, corresponding to the area size of 0.96 mm x 0.77mm, 1.28 mm x 1.02 mm, and 14mm x 11mm, with the spatial resolution of 3.0 μm x3.0 μm, 4.0 μm x 4.0 μm, 43 μm x 43 μm, respectively. The frame rate for taking an image was selected 60 ~ 1000 frames/s (16.7msec~1msec per one picture) in this study. The length and distortion are calibrated by using a standard micro-scale of USAF 1951. The intensity was calibrated with the 82ch data logger by measuring the electric current of temperature sensor.

2.2 A precision temperature control of a micro alignement specimen stage

Temperature control of a micro precision alignment xyz stage with a pitch of 1μm was electronically designed by using a FPGA (Xilinx) technology. A constant rate of heating and cooling, 0.1°C/min-500°C /min is routinely used for thermal analysis in a thermo-graphical view.

2.3 n-alkanes

The n-alkanes examined in this studied are n- pentacosane ($C_{25}H_{52}$), n- tetracosane ($C_{24}H_{50}$), and n-tricosane ($C_{23}H_{48}$). The crystallographic structures of the rotator phase determined in X-ray diffraction are as follows.

1. *n* - pentacosane, $C_{25}H_{52}$ (crystal systems : orthorhombic -> hexagonal -> liquid)
2. *n* - tetracosane, $C_{24}H_{50}$ (: monoclinic -> hexagonal -> liquid)
3. *n* - tricosane, $C_{23}H_{48}$ (: triclinic -> hexagonal -> liquid)

http://dx.doi.org/10.21611/qirt.2008.10_06_07

3. Analytical procedure

i) Time differential

Time differential images are calculated from

$$I'(t) = \frac{\partial I}{\partial t} = \lim_{\Delta t \to 0} \frac{I(t) - I(t - \Delta t)}{\Delta t}$$

where I (t) is intensity, t is time, Δt is time interval between the capturing. A time differential filter was used to obtain the time differential image by selecting an optimum matrix size.

ii) Discrete-time Fourier transform,

$$G(\frac{n}{N}) = \frac{1}{N} \sum_{K=0}^{N-1} g(k) \exp\left(-j 2\pi nk / N\right)$$

where G(n/N) is a discrete Fourier transformed function, and N is a sample number in one cycle.

4. Results and discussion

4.1 *n* - tetracosane, $C_{24}H_{50}$

Fig.1 shows a differential thermal analysis (DTA) curve in a cooling scan from the molten state (60°C) to the solid state (20°C) of *n*-alkane $C_{24}H_{50}$. The exothermic heat is observed at the crystallization (b, c, d) and the rotator phase transitions (f). The time indicated by each arrow in Fig. 1 corresponds to the thermo graphic images (b, c, d, f) and the time differential three-dimensional images (a, e) in Fig.2, in which the position for DTA analysis is indicated as a black arrow. The developing process of crystalline lamellae is observed in Fig.2b-d, succeeded by the rotator phase transitions in Fig.2f. On the other hand, the 3D differential images in Fig.2a and e show the spatial temperature

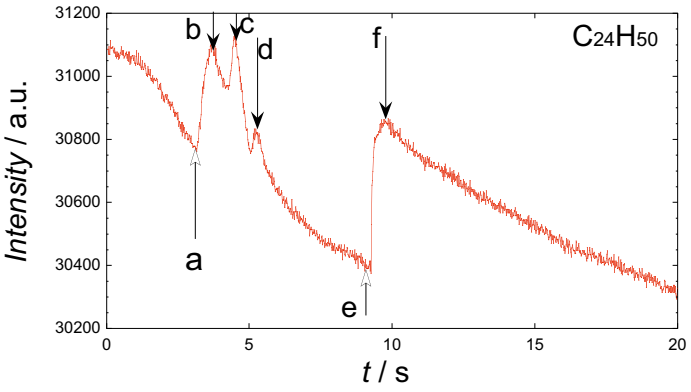

Fig. 1. Time development of a photon-count intensity detected on a selected pixel (shown as a black arrow in Fig.2) of IR-FPA in the process of crystallization and rotator phase transition of $C_{24}H_{50}$ in a rapid cooling (-60°C/min) measurement.

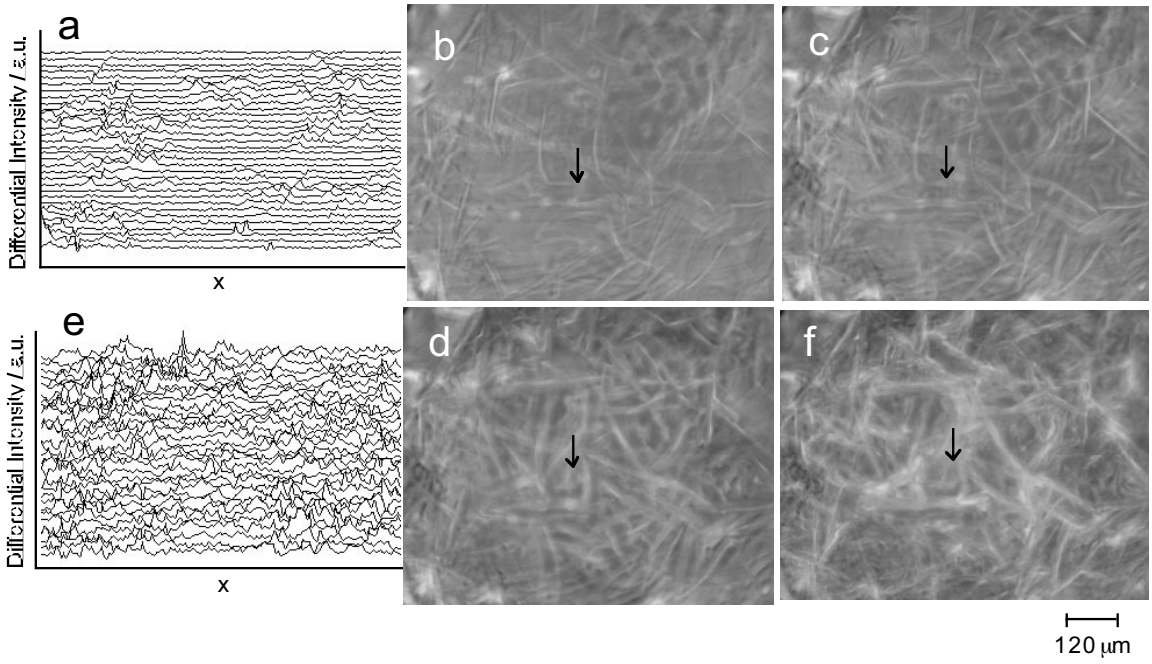

Fig. 2. Differential images of temperature distribution at the moment of (a) crystallization and (e) rotator phase transition. IR microphotographs in the process of crystallization (b, c, d) and rotator phase transition (f) of $C_{24}H_{50}$ in a rapid cooling measurement. Alphabets correspond to the arrows in Fig.1.

http://dx.doi.org/10.21611/qirt.2008.10_06_07

fluctuation a moment before an occurrence of crystallization and rotator phase transition, which affects the structure developing process. For example, in the liquid-solid phase transition in Fig. 2a the temperature fluctuation is localized in contrast to the rapid and homogeneous fluctuations observed in solid-solid phase transition in Fig.2e.

Taking into account the thermal diffusivity of $C_{24}H_{50}$ in between phase transitions, measured by a temperature wave method [5], one of the reasons for this phenomenon can be explained. Thermal diffusivity of $C_{24}H_{50}$ shows a step increase from the liquid to hexagonal, and to monoclinic crystal systems. The phase transitions in Fig. 2a, and 2e started on the different basis of thermal diffusivity, $0.8 \times 10^{-7} m^2 s^{-1}$ in the liquid state (Fig. 2a), and $1.25 \times 10^{-7} m^2 s^{-1}$ in the hexagonal crystal state (Fig. 2e).

With an advantage of the small amount of specimen, the time and spatial differential analysis of high-speed thermography gives the precise information of the structure developing process in view of the heat transfer and thermal properties.

4.2 *n* - pentacosane, $C_{25}H_{52}$

The process of growth of a crystalline lamella of odd number *n*- alkane $C_{25}H_{52}$ under a cooling scan is clearly observed by the micro-scale IR system with a high magnification lens. Fig. 3 shows a time differential IR image measured in the crystallization (Fig. 3 a) and a rotator phase transition (Fig.3b, c). A bright-color part corresponds to the edge front of exothermic heat on lamella formation. In the same manner as observed in Fig. 2 the different exothermic heat patterns are seen in the crystallization and the rotator phase transition. In crystallization (Fig. 3a) a spindle-shaped crystalline lamella is formed one by one, on the other hand, in rotator phase transitions (Fig. 3b, c) the exothermic heat front proceeds instantaneously.

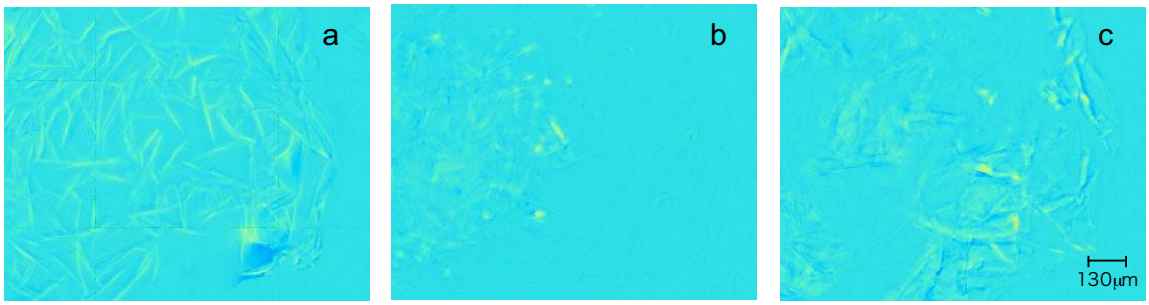

Fig. 3. Differential images of exothermic heat front of crystalline lamellae; (a) crystallization (liquid state to hexagonal state), (b) rotator phase transitions, and (c) rotator phase transition (hexagonal to monoclinic) in a rapid cooling measurement (-60°C/min) of $C_{25}H_{50}$.

The spindle-shaped lamellae size is about 20μm wide and 160μm long. The magnified image of lamellae (in hexagonal state) is shown in Fig. 4. The lamellae are appeared randomly at first, and then stacked and overlapped with each other, in the appearing order of 2 – 1 – 3 – 5 – 7, as schematically shown in Fig. 4c. The early stage of appearance of lamellae No. 1-5 is shown in Fig. 5 with the time differential IR images at every 16.7ms. Lamella 2 appears first, then lamella 1 and 3 starts to grow, and then they spread into branches.

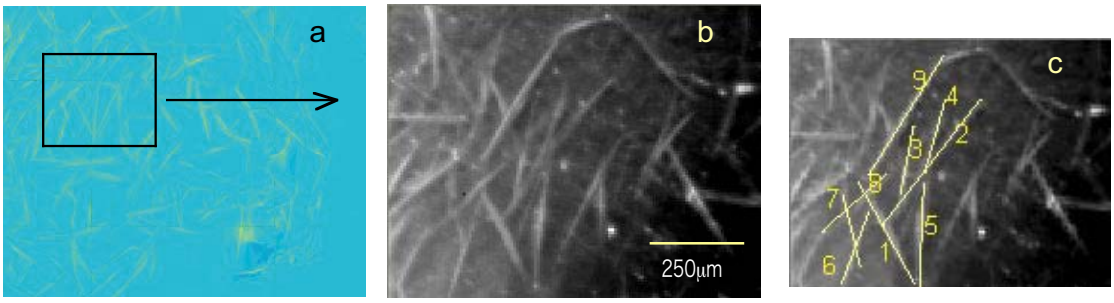

Fig. 4. The encircled area with a frame in the differential image on crystallization of $C_{25}H_{50}$ (a) is magnified as an IR image of lamellae in (b). The lamellae are numbered 1-9 in (c).

Fig.5

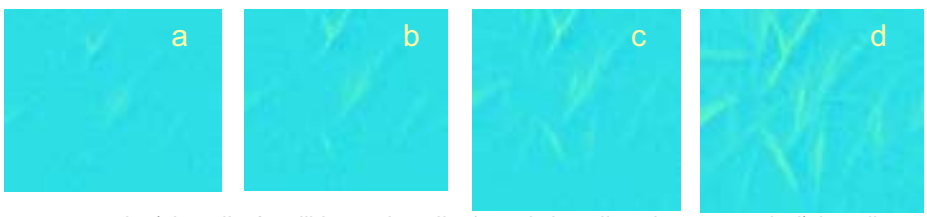

The lamella growth process observed by a differential IR image.
a) lamella 2 is appeared, b) lamella 1 and 3 are appeared, c) lamella 2 collides to lamella 1, and lamella 5 is appeared, d) lamellae are in growth in different branches.

The micro-scale thermal analysis of each lamella No.1-5 can be done with in situ analysis of intensity profiles under cooling scan with the images of Fig. 3-5. The thermal analysis along the growth direction (long axis) of lamella No. 1 and 2 is shown in Fig. 6.a,b.

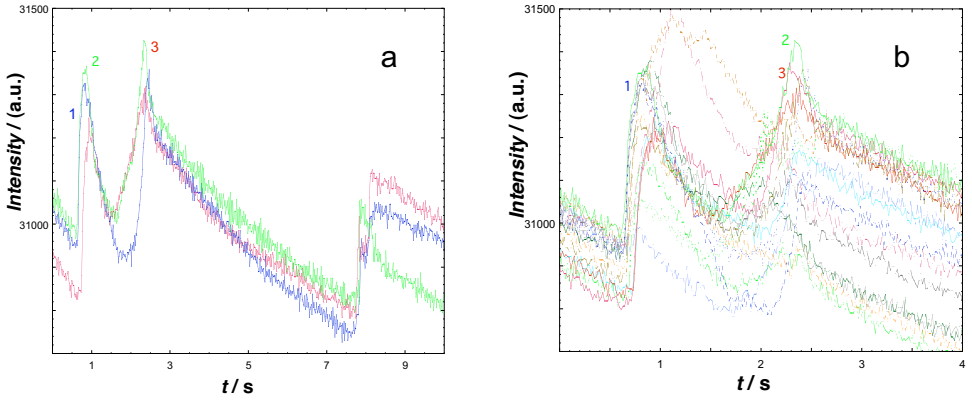

Fig. 6 On-lamella thermal analysis of lamella 1 in a different time scale for crystallization and phase transitions; (a) in the long time range, and (b) in the shorter time range.

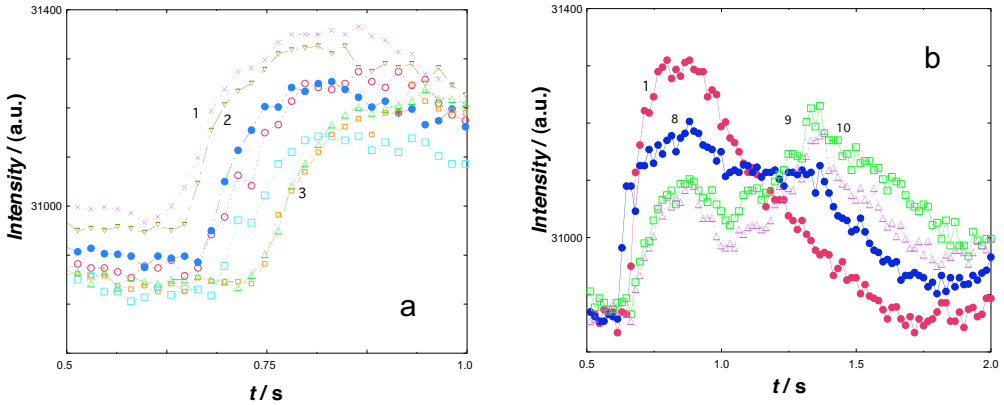

Fig. 7 The early stage of lamella 1 growth in different directions by the on-lamella thermal analysis. (a) along the long axis (in the direction of the lamella growth) and (b) in the perpendicular direction to the long axis of the lamella1 growth.

The typical intensity profiles of lamellae 1 show three peaks, which correspond to the three different exothermic heat patterns as observed in Fig. 3. The 1st peak corresponds to the liquid-solid phase transition (crystallization), and the 2nd and 3rd correspond to the solid-solid phase transitions (rotator phase transitions). The early stage of crystallization of lamella 1 is re-plotted in Fig. 6b. The different profiles can be seen on each different pixels on lamella 1, which indicates that the inter-correlation of lamella 1 with the surrounding temperature field is not simple. Different from the case observed in the biological cells[1]-[4] , the structure (crystalline lamella) is newly formed in the temperature field with exothermic heat.

In Fig. 7 much earlier stage of crystallization is analyzed in two different directions, in the growth direction of lamella 1 (Fig. 7a) and in the perpendicular direction to it (Fig. 7b). The time delay of its rising part of the 1st peak in Fig. 7a corresponds to the lamella growth in the long axis direction at each located pixel on lamella 1. The edge front of the lamella grows from the center to the both end, but and only one DTA peak can be found in this direction. On the other hand, in the thermal analysis in the perpendicular direction (Fig. 7b), a shifted peak is appeared definitely before the occurrence of rotator phase transition. This 2nd peak is found as correlated with the widening of lamella1 in the perpendicular direction to the long axis of the lamella growth. It is noteworthy to mention that the micro-scale thermal analysis by IR image can detect the anisotropic lamella growth with time delay in different directions.

4.3 *n* - tricosane, $C_{23}H_{48}$

The exothermic heat patterns of odd number n- alkane $C_{23}H_{48}$ is different from that of $C_{25}H_{50}$. The spindle-type straight lamella formation is not observed in the crystallization, but a dot-like image can be observed in the time differential pattern (Fig. 8a). On the other hand, in the rotator phase transition a straight shaped lamella is clearly appeared (Fig. 8b), but in a sparsely manner. In addition, a re-crystallization of lamellae is clearly observed under a heating scan from the triclinic to the hexagonal phase (Fig. 8c). This unique growth pattern of exothermic heat is attributable to the β phase in hexagonal crystal of $C_{23}H_{48}$ that can be found by temperature wave analysis [5,6].

The profile of micro-scale thermal analysis on lamella No.10 (Fig. 9b), which is formed in the solid-solid phase transition from the hexagonal to triclinic phase, is shown in Fig. 9a. In this case the lamella is more isolated (Fig. 9b) and the temperature field outside the lamella can be analyzed. No exothermic heat influence can be detected

http://dx.doi.org/10.21611/qirt.2008.10_06_07

in the distance of 3 – 4 pixels from the lamella (lines No. 1 & 2 in Fig. 9a), less than 15 μm in this case. The exothermic heat of biological cells was more influential in the longer distance (in the range of 40 – 50 μm) and this information would be helpful to evaluate the correlation matrix in the inverse problem numerical analysis to determine the heat source term by the method of Cristophe et al. [7].

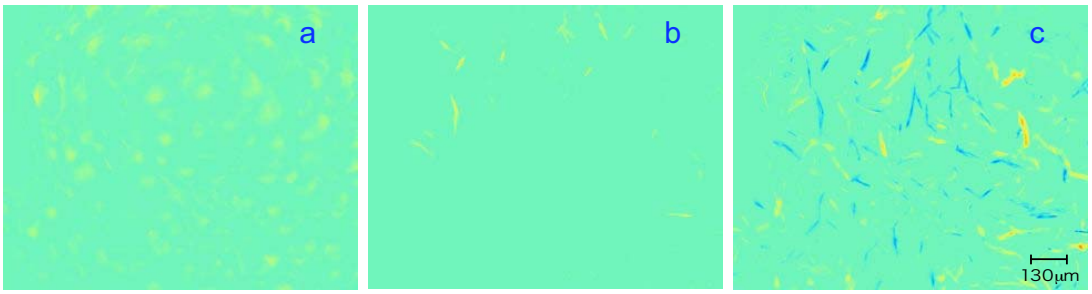

Fig. 8 Differential images of exothermic heat pattern in (a) crystallization, (b) rotator phase transition in cooling (-20°C/min), (c) rotator phase transition in heating (+20°Cmin) of $C_{23}H_{50}$.

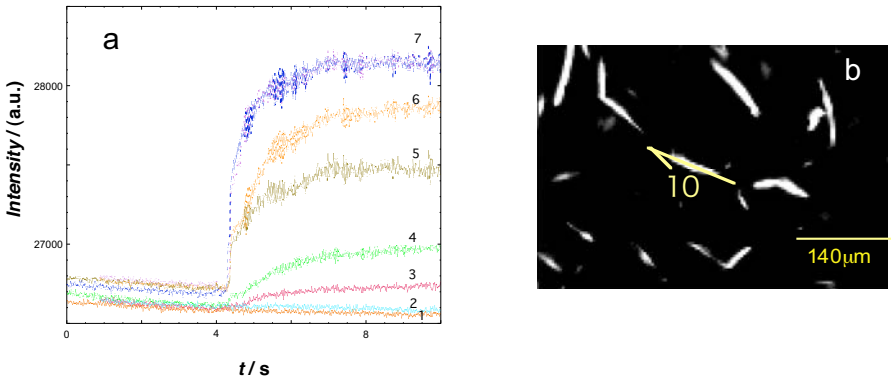

Fig. 9 (a) The intensity profiles in the growth process of lamella No.10 on the pixels along the direction of the arrow indicated in Fig. 9b, (b) IR image of an isolated lamella of $C_{23}H_{48}$ that is appeared in the rotator phase transition in cooling,

5. Conclusion

The exothermic heat patterns of the lamellae growth of *n*- alkane during phase transitions were obtained by the high-speed micro-scale IR imaging technique. The odd-even number effect of rotator phase transition was observed by the different exothermic heat pattern. It gives us a new insight to understand the lamellae growth process of phase transitions in micro-scale. To summarize the main point of this paper is as follows.

1. On-lamella micro-scale thermal analysis is shown on the odd and even number n-alkane.
2. The odd-even number difference of the exothermic heat patterns on phase transitions is shown by the time differential exothermic heat pattern in micro-scale.
3. The anisotropic growth rate of the crystalline lamellae is found in the width and the length directions.

The micro-scale thermal analysis of IR camera has an advantage to observe the direction of diffusion of exothermic heat and this technique can be applied to various fields of material sciences in combination with the numerical data analysis of the inverse problem.

REFERENCES

[1] T. Hashimoto, and J. Morikawa, Two-dimensional thermal analysis on freezing of onion epidermal cell by high-speed infrared microscopic camera, *Jpn. J. Appl. Phys.,* 42 (2003) L706-L708.
[2] J. Morikawa, T. Hashimoto, E. Hayakawa, H. Uemura, Two-dimensional thermal analysis for freezing of plant and animal cells by high-speed microscopic IR camera, SPIE, 5073 (2003) 148-153.
[3] J. Morikawa, T. Hshimoto, K.Yamamoto, J. Ando, Tow-dimensional thermal analysis for freezing of endothelial cells by high-speed microscopic IR focal plane arrays, SPIE, 5697 (2007) 282-290.
[4] J. Morikawa, T.Hashimoto, E. Hayakawa, T. Eto, Two-dimensional thermal analysis of organic materials by IR thermography, QIRT Congress, Padova, 2006.
[5] N. Miyamoto, J. Morikawa, T. Hashimoto, Thermal diffusivity of Binary mixture of *n*-tricosane and *n*-tetracosane by Fourier Transform Temperature Wave Analysis, Thermochim. Acta 431 (2005) 62-67.
[6] J. Morikawa, T. Hashimoto, Simultaneous measurement of heat capacity and thermal diffusivity in solid-solid and solid-liquid phase transitions of n-alkane, *Thermochim. Acta*, 352-353, (2000) 291-296.
[7] C. Pradere, M.Joanicot, J.C. Batsale, J. Toutain, C. Gourdon, Processing of temperature field in chemical microreactors wuth infrared thermography, QIRT J. Vol. 3 No.1 (2006) 117-135.

http://dx.doi.org/10.21611/qirt.2008.10_06_07